J Mater Sci (2008) 43:7157–7164
DOI 10.1007/s10853-008-3022-2

Effect of Ce and La on microstructure and properties of a 6xxx series type aluminum alloy

Mehdi Hosseinifar · Dmitri V. Malakhov

Received: 12 June 2008 / Accepted: 26 September 2008 / Published online: 23 October 2008

Abstract The increase in iron content in secondary sources of aluminum has led to an increase in the amount of Fe-bearing intermetallic phases in Al alloys. One of these intermetallics, β-AlFeSi, which is seen as the dominant phase in 6xxx series alloys, reduces bendability of wrought alloys, which in turn, limits their usage in the automotive industry. It is known that small additions of Sr prevent the formation of the β phase and facilitate the precipitation of a less detrimental intermetallic, α-AlFeSi, in as-cast alloys. It is worth investigating whether other elements cause a similar effect. Cerium and lanthanum as the least expensive representatives of rare-earth metals are tried as such elements. It is found that in alloys containing 0.1–0.2 wt.% of lanthanum, the fraction of β particles is pronouncedly less than that in the reference alloy. In addition to this advantage, much smaller grains are seen in the alloy with 0.2 wt.% La. Despite similarities between La and Ce, the latter metal neither modifies the microstructure nor noticeably affects the grain size. Moderate thermo-mechanical processing nullifies the beneficial effect of small La additions resulting in no improvement in the bendability of the alloy.

Introduction

6xxx series aluminum alloys combining a high strength-to-density ratio and a good corrosion resistance are candidates for manufacturing automotive body panels. These panels are usually two layer structures, in which an outer layer is joined to an inner one by a hemming operation. Such operation involves small radius bending of the outer panel. Aluminum sheet alloys used for this application must have an adequate bendability.

Currently, one of the principal barriers to improved Al alloy sheet bendability is the presence of relatively brittle intermetallic particles distributed throughout the structure. These particles can induce damage and premature failure in a wide variety of sheet forming and bending operations. This detrimental behavior is particularly acute in sheets prepared by strip-casting, a cost-effective processing method that is otherwise well-suited for automotive Al alloys [1, 2]. Furthermore, with the ever increasing use of recycled scrap aluminum, greater levels of Fe-bearing intermetallic particles must be tolerated if prohibitively expensive purification processes are to be avoided.

In the 6xxx series Al alloys, the presence of iron is manifested via the formation of two major intermetallic compounds: β-AlFeSi (monoclinic, plate-like) and α-AlFeSi (cubic, Chinese script). β is the dominant phase in the cast microstructure of 6xxx series Al alloys. The undesirable shape of β particles and their brittleness are claimed to reduce the formability of these alloys. In contrast, it is shown that the presence of α instead of β has resulted in improved ductility and extrudability of the alloy [3–6]. In this respect, it might be possible to improve the bendability of the 6xxx series Al alloys if α becomes the dominant Fe-bearing phase. It is possible to promote the formation of α in several ways. It has been shown that homogenization treatment of alloys at 580 °C for 6 h transforms a majority of β formed during solidification to α [7, 8]. This procedure, however, is costly. Alternatively, the formation of α can be promoted during solidification by the addition of modifying elements.

M. Hosseinifar (✉) · D. V. Malakhov
Department of Materials Science and Engineering, McMaster University, 1280 Main St. W., Hamilton, ON, Canada L8S 4L7
e-mail: hossem@mcmaster.ca

Strontium is a well-studied example of such elements [9–12]. A small addition of Sr to 6xxx series Al alloys favors the formation of the α-AlFeSi phase rather than the β-AlFeSi intermetallic phase. However, the high price of Sr and the fact that its utilization increases the amount of dross severely restricts its usage in practice.

In a search for less expensive modifying elements, rare-earth metals (REM) seem to be good candidates. It was reported in literature that small additions of REM had a beneficial effect upon ductility of magnesium alloys [13, 14], lead-free solders [15, 16], iron aluminides [17, 18], and Fe–V–W–Mo alloys [19]. The effect was attributed to smaller grain sizes, more finely dispersed second phase particles, and smaller aspect ratios of the particles. Furthermore, an ability of mischmetal (a mixture of REM) to affect the microstructure of aluminum alloys in general, and the morphology of iron-bearing intermetallics in particular, has also been reported in literature [20, 21].

In the present study, cerium and lanthanum were chosen to be added to an experimental 6xxx series Al alloy since they were the cheapest among the 17 members of the REM family. It is worth noting that these two elements together comprise approximately 90% of mischmetal. The modifying effect of these elements on the iron-bearing intermetallics and grain structure of the alloy in as-cast and T4 conditions was examined qualitatively and quantitatively. Tensile testing was performed on samples in T4 condition to assess possible improvements in the bendability of the alloy.

Experimental

Materials

An experimental aluminum alloy with 0.7 wt.% Mg, 0.7 wt.% Si, 0.2 wt.% Cu, and 0.45 wt.% Fe was used in the present investigation. The concentration of iron was higher than that observed in typical 6xxx series Al alloys. It was done deliberately in order to stimulate the formation of the Fe-bearing intermetallics and see more clearly the "healing effect" of Ce and La if such effect did exist. Varying amounts of Ce and La from 0.03 wt.% to 0.2 wt.% were added to the above reference alloy to prepare two series of alloys. More than 0.2 wt. % can hardly be classified as a "small amount". The minimum amount of 0.03 wt. % was chosen to compare the modifying power of cerium and lanthanum with that of Sr, for which 300 ppm worked [10]. The composition of these alloys as verified by glow discharge optical emission spectroscopy is presented in Table 1. Properties and microstructures of samples with Ce and La additions were compared with those of their respective reference alloys, RC and RL.

Table 1 Chemical compositions of alloys used in the present work (wt.%)

Alloy	Mg	Si	Fe	Cu	Ce	La
RC	0.76	0.8	0.5	0.21	–	–
C04	0.79	0.81	0.53	0.23	0.04	–
C07	0.75	0.76	0.5	0.21	0.07	–
C1	0.79	0.85	0.55	0.23	0.1	–
C2	0.75	0.78	0.51	0.22	0.2	–
RL	0.82	0.56	0.42	0.2	–	–
L04	0.83	0.57	0.43	0.2	–	0.04
L07	0.81	0.57	0.43	0.2	–	0.07
L1	0.85	0.6	0.45	0.2	–	0.11
L2	0.8	0.58	0.42	0.19	–	0.21

Casting and processing

Commercial purity aluminum containing 0.13 wt.% iron was melted in a graphite crucible placed in a pit-type electrical resistance furnace. Si, Mg, Fe, Cu, and REM were added as pure materials. A flow of argon was used to remove hydrogen and thus minimize hydrogen-induced porosity. Argon was injected into the bottom of the crucible through a rotating tube which also stirred the melt. For each composition, two $5 \times 5 \times 25$ cm^3 ingots were produced by pouring the melt in a water-chilled copper mold.

In industrial practice the forming process is performed on the sheets in T4 temper or pre-aged condition before the final aging during paint bake [22]. This practice was used as a guideline in the present investigation. Alloy sheets were prepared by hot-rolling samples at 430 °C from 8 mm in thickness to 3 mm, which corresponds to 62% reduction. Rolled samples were solutionized at 570 °C for 2 h and quenched in ice water. The quenched samples were brought to T4 temper by natural aging at room temperature for at least 14 days and then tested.

Microstructural analysis and mechanical testing

To avoid center line and edge effects, 1.4×1.4 cm^2 of the center and 0.8 cm of the edges of the ingots were discarded and the remaining sections were used for experiments. Scanning electron microscopy (SEM) and energy-dispersive spectroscopy (EDS) were used to characterize the morphology of intermetallic compounds and estimate their chemical composition. Intermetallic particles were extracted from alloys in as-cast and T4 temper via a selective dissolution of the FCC matrix in boiling phenol and identified by X-ray diffraction (XRD) analysis. The details of the extraction procedure are explained elsewhere [23]. To reveal the true 3D morphology of intermetallic particles,

$0.75 \times 0.75 \times 3$ cm^3 samples were held in boiling phenol for 5 min and examined by SEM.

The effects of Ce and La were quantified via morphological changes of Fe-bearing intermetallic compounds. Quantitative metallography was employed to determine the area % of intermetallic phases. For each alloy, six SEM images taken in the backscatter mode were analyzed by UTHSCSA ImageTool 3 image analyzing software.[1]

A characterization of the grain size of as-cast and T4 tempered alloys electroetched in Barker's reagent was performed according to the ASTM E112-96 standard.

A common method of assessing bendability is to measure the *r/t* ratio, where *r* is the minimum bend radius attained without fracture and *t* is the sheet thickness. The smaller the (*r/t*) value, the greater the bendability of a material. Datsko and Yang [24] theorized that "failure will occur in the outer fiber of a material being bent when the true strain in the outer fiber is equal to the true strain at the instant of fracture of a tensile test specimen of the same material". They proposed the following relation,

$$\frac{r_{\min}}{t} = \frac{C}{A_r} - 1 \quad (1)$$

where C is a constant equal to 50–60 and A_r is reduction in area at fracture in a tensile test expressed in percentage. They showed that this relation properly correlated the experimentally measured bendability data to A_r for different materials. It means that the bendability of a material can be assessed by a simple tensile test.

In order to assess the bendability of the alloys studied, tensile test specimens were machined from the sheets in T4 temper according to ASTM B557 (subsize specimen 1 inch gauge length). In each case, four samples were tested by an Instron 5566 machine; a constant crosshead speed of 2 mm/min was maintained. A strain gauge extensometer was employed to measure the elongation with a great deal of accuracy.

Results and discussion

As-cast condition

Figure 1 shows a typical cast microstructure of the reference alloy sample. The microstructure consists of primary aluminum and AlFeSi intermetallic particles. According to the results of the EDS examination the Fe/Si ratio in these particles is very close to one. The composition of one of these particles arrowed in Fig. 1 is presented in Table 2. The Fe/Si ratio close to unity corresponds to the β-AlFeSi phase the stoichiometric formula of which is either Al_5FeSi [10] or $Al_9Fe_2Si_2$ [25, 26]. The X-ray diffractogram of intermetallics extracted from this sample as shown in Fig. 2 corroborates that these particles consist of

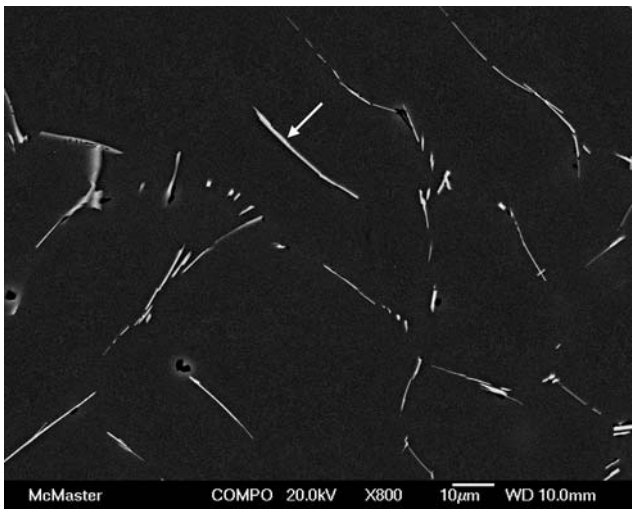

Fig. 1 Backscattered image of as-cast reference alloy RC, showing that the β phase platelets (seen as needles) are the only intermetallic particles present in the microstructure

Table 2 EDS analysis of the composition of the particle arrowed in Fig. 1

Element	Atomic% (±0.1)
Al	81.7
Si	9.1
Fe	9.2

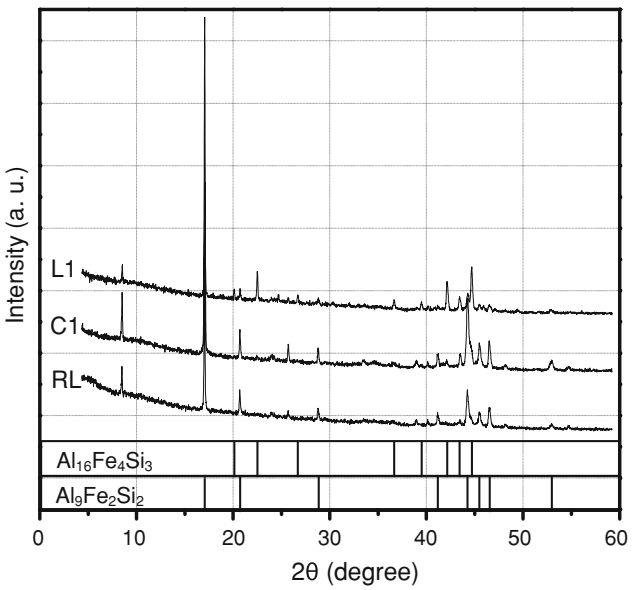

Fig. 2 XRD patterns of intermetallic phases extracted from as-cast RC, C1, and L2 alloy samples

[1] http://ddsdx.uthscsa.edu/dig/itdesc.html.

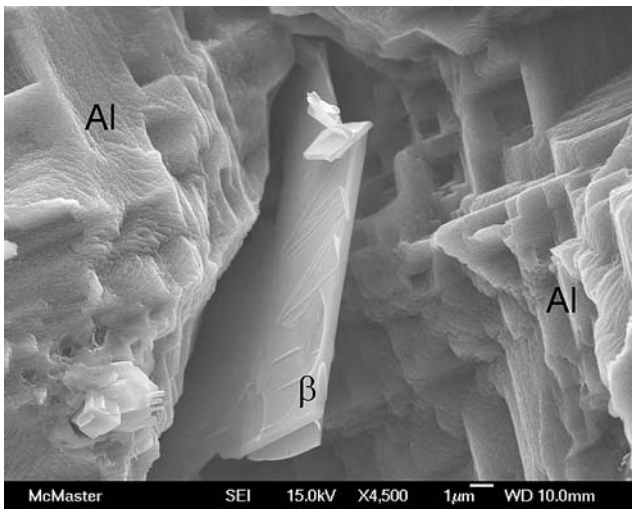

Fig. 3 SEM micrograph showing the morphology of the β-AlFeSi phase in the as-cast reference alloy RC

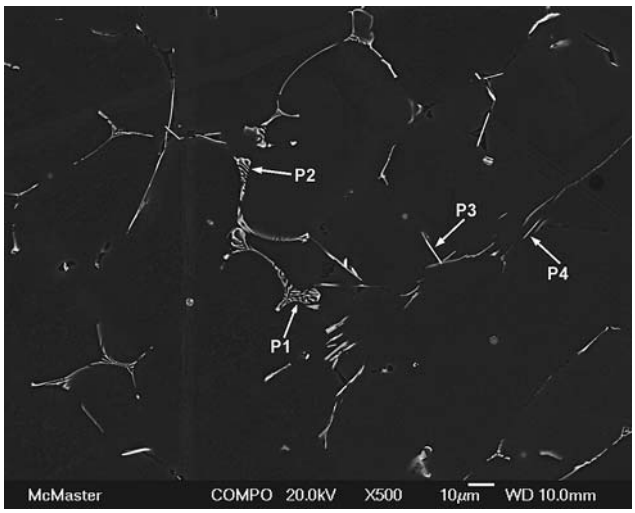

Fig. 4 SEM image of L1 alloy showing Chinese script α (P1 and P2), plate-like β (P4), and La-containing (P3) intermetallic particles

monoclinic $Al_9Fe_2Si_2$. The two-fold symmetry of the monoclinic structure forces a two-dimensional growth of the β particles [27, 28] which means that needle-like particles seen in Fig. 1 are plates in 3D space. Figure 3 showing the reference sample with the FCC matrix partially dissolved in boiling phenol (deep etching) proves this to be the case.

Additions of cerium did not noticeably change the phase portrait of the alloy. As shown in Fig. 2 the XRD spectrum of extracted particles from the sample containing 0.1 wt.% Ce is very similar to that of the reference sample. This observation was made for all Ce-containing alloys. As an advantage, however, Ce was able to slightly decrease the aspect ratio of β particles (Table 3).

An addition of La up to 0.07 wt.% also did not change the type of the constituent phases in the as-cast alloys. An interesting change in the nature of intermetallics was observed for alloys with 0.1 and, more pronouncedly, with 0.2 wt.% of lanthanum in which particles with Chinese script morphology existed side-by-side with the β particles.

Table 4 EDS analysis of the composition of the particles P1 through P4 shown in Fig. 4

Element	Atomic% (±0.1)			
	P1	P2	P3	P4
Al	80.1	77.2	71	83.3
Si	8.3	8.4	14	8.4
Fe	10	13.2	–	8.3
La	–	–	5	8.4
Cu	1.6	1.2	1.8	8.3
Mg	–	–	8.2	2

The SEM micrograph of a sample containing 0.1 wt.% La presented in Fig. 4 evinces the presence of this morphology of iron-containing intermetallics. According to the outcome of an EDS analysis summarized in Table 4, these particles were characterized by a Fe/Si ratio within the 1.2–1.6 range. XRD spectrum of the particles extracted from this sample identified this phase as cubic α-$Al_{16}Fe_4Si_3$. By

Table 3 Effect of Ce and La on the intermetallic phases

Alloy	Total area percent of intermetallic Phases ($\alpha + \beta$)	Area percent of α phase	Aspect ratio of β particles
RC	2.11 ± 0.06	–	7.0 ± 0.3
C04	2.28 ± 0.08	–	6.3 ± 0.4
C07	2.32 ± 0.10	–	6.5 ± 0.2
C1	2.34 ± 0.10	–	5.7 ± 0.1
C2	2.47 ± 0.20	–	5.4 ± 0.2
RL	2.05 ± 0.07	–	6.1 ± 0.2
L04	2.13 ± 0.05	–	6.0 ± 0.2
L07	2.19 ± 0.20	–	5.3 ± 0.2
L1	2.22 ± 0.20	1.17 ± 0.09	5.3 ± 0.1
L2	2.4 ± 0.07	1.84 ± 0.10	5.2 ± 0.1

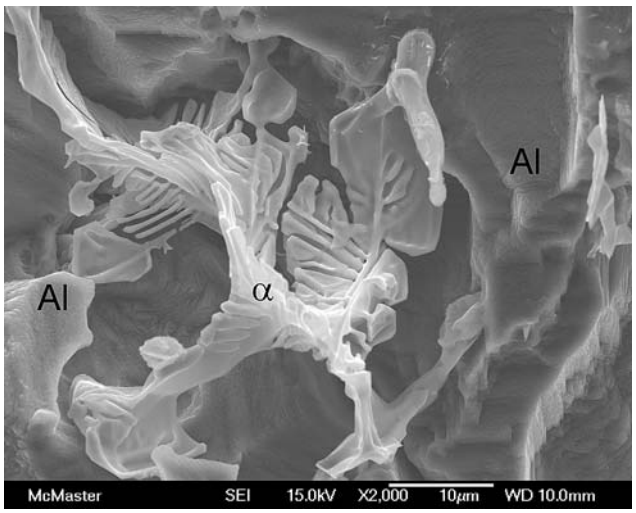

Fig. 5 Three-dimensional morphology of an α-AlFeSi intermetallic particle observed in L2 alloy (containing 0.2 wt.% La)

raising the concentration of La from 0.1 wt.% to 0.2 wt.%, the fraction of the α phase can further be increased from 1/2 to approximately 3/4.

The 3D shape of these particles was revealed by deep-etching a sample containing 0.2 wt.% La (Fig. 5). The cubic crystal structure of α allows it to grow in all 3 dimensions resulting in its irregular shape.

A possible mechanism proposed for Sr addition considers the solidification sequence leading to the formation of β. It is thought that β particles mainly form at the expense of α by the following peritectic reaction [29, 30]: $L_1 + Al_8Fe_2Si\ (\alpha) \rightarrow L_2 + Al + Al_5FeSi\ (\beta)$, where L_1 and L_2 and are liquids with different compositions.

Mulazimoglu et al. [10] found a silicon-rich layer around α particles in the presence of Sr. This suggested that a barrier at the interface prevented Si penetration into the α particle. Consequently, the peritectic reaction leading to the formation of β was suppressed. They proposed that Sr adsorbed to the α/L interface during solidification and acted as this barrier.

It is reported that the addition of over 0.2 wt.% manganese also promotes the formation of the α phase [31, 32]. The mechanism by which Mn stabilizes α is different than that proposed for Sr. In the former case, α becomes a quaternary phase in which Fe and Mn share the same sublattice. The presence of Mn and Fe in one sublattice increases the entropy contribution to the Gibbs energy of the phase and hence increases its stability [23].

Solid-state solubility of lanthanum in aluminum is very low. During solidification, La accumulates in the melt and may affect the formation of iron-containing intermetallics by either of the mentioned mechanisms. Examination of several plate-like and Chinese script Fe-bearing intermetallics using EDS did not reveal the presence of La in them which pointed out to the surface adsorption as a more plausible mechanism. It is deemed that adsorption of La to α/L interface, similar to Sr, does not allow Si to enter α, thus preserving its dominance in the as-cast microstructure.

La, however, did participate in the formation of new intermetallic particles. An example of such particles is P3 in Fig. 4. The presence of La which has a high atomic weight makes these particles seem brighter than Fe-bearing intermetallics. It must be noted that this new phase does not contain iron (refer to the composition of particle P3 presented in Table 4). This was also the case in Ce-added alloys where Ce-bearing particles with no iron inside were observed. There is a slight increase in the total area % of intermetallics with the increase in the amount of Ce and La (Table 3). This increase can be attributed to the formation of these new Ce- or La-containing phases.

Another evidence for the greater modification power of lanthanum was gained by examining the grain structure of

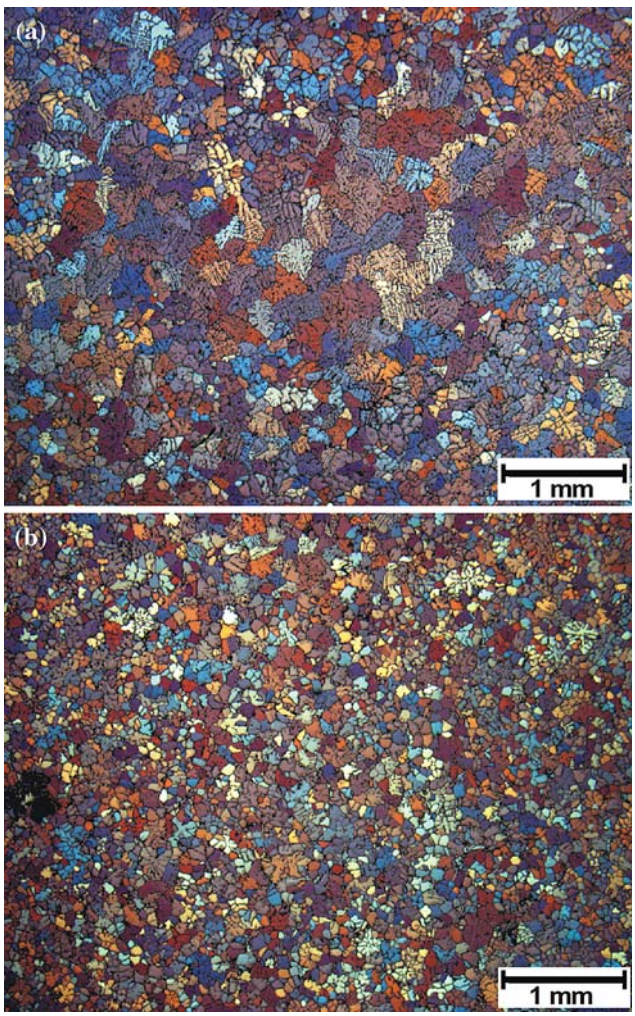

Fig. 6 Grain structure of **a** as-cast C2 alloy sample, showing a non-uniform structure and **b** as-cast L2 alloy sample, showing a uniform grain size

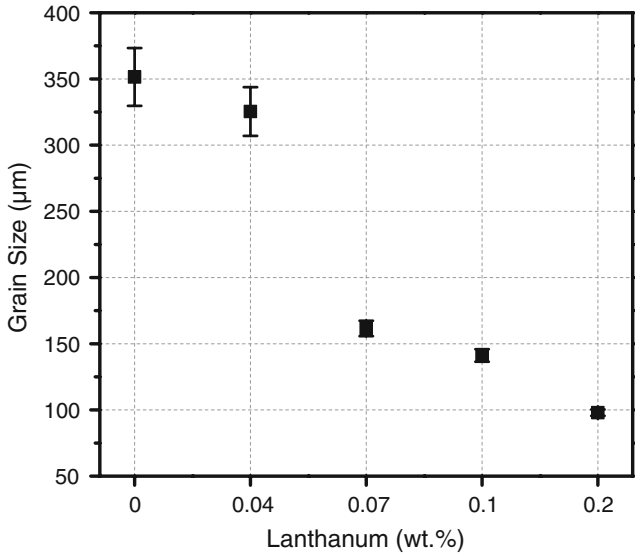

Fig. 7 Influence of La on the grain size of as-cast alloys

the alloys. The grain structure of samples with 0.2 wt.% Ce and 0.2 wt.% La are compared in Fig. 6a and b. It is seen that the addition of 0.2 wt.% cerium results in a non-uniform grain structure, while the La-added sample shows a uniform grain size. The same non-uniformity of grain structure was also seen at lower Ce concentrations. More importantly, the increase in La content resulted in a gradual decrease in the grain size of the cast alloy (Fig. 7). The cause of this phenomenon is under investigation.

At first glance, both a smaller grain size and a greater fraction of α-AlFeSi particles with Chinese script morphology are beneficial to the formability of the Al alloy under investigation. However, it should be kept in mind that 6xxx series alloys are wrought heat-treatable alloys and, therefore, a favorable alteration of the as-cast microstructure is practically meaningful only if the effect of this alteration is retained in alloys which have undergone thermo-mechanical processing.

T4 condition

Uniaxial tension test was performed on reference, C1, and L2 alloy samples in T4 temper and tensile properties data were extracted from stress–strain curves. It is seen in Table 5 that all pertinent properties are virtually the same. Since the alloys show the same elongation at fracture, Eq. 1 predicts that all alloys have the same level of bendability. It means that, despite all the beneficial effect that the addition of La has had on the alloy in as-cast condition, it has not been able to deliver the sought-after higher bendability of this alloy. The microstructure and grain size of the alloys in T4 temper were examined to explain the cause of this phenomenon.

The microstructures of the reference, C1, and L2 alloys in T4 temper are illustrated in Fig. 8a–d. It is seen that morphological features of the cast alloys have changed considerably after thermo-mechanical processing. The Fe-containing intermetallics have broken down into relatively smaller parts. On the other hand, rolling and solutionizing have had little influence on the type of the AlFeSi phases. XRD examination showed that β-AlFeSi was still the dominant intermetallic phase in reference and C1 alloys while α-AlFeSi was the dominant phase in L2 alloy. The important observation is that the microstructures of all alloys are now similar, exhibiting relatively small-sized and discrete AlFeSi particles forming a necklace-type configuration.

It is known that the adverse ability of brittle intermetallic phases to initiate voids and consequently induce damage is proportional to their size. Image analysis investigation of particles after thermo-mechanical processing showed that the average size of particles is about 2 μm in all alloys. This can explain why L2 alloy does not have superior bendability over reference and C1 alloys.

The grain size measurement of the samples in T4 temper also showed no difference between the reference and La-added samples (Table 6). It is apparent that dynamic recrystallization accompanying hot rolling followed by grain growth during solutionizing has eliminated the grain refinement caused by La addition seen in the as-cast case. This observation provides another explanation for the same bendability observed for all alloys.

It is seen that the advantageous effects of La on as-cast alloys do not hold after their moderate deformation and solutionizing. However, it does not mean that the La addition is completely fruitless. The effect of microstructural changes in as-cast stage on the intermediate processes should not be underestimated. Paray et al. [11] examined

Table 5 Tensile properties of samples in T4 temper

Alloy	Yield stress (MPa)	Ultimate tensile stress (MPa)	Uniform elongation (%)	Elongation at fracture (%)
RC	124 ± 1	240 ± 1	20 ± 1	23 ± 1
C1	128 ± 3	239 ± 2	21 ± 1	25 ± 2
RL	128 ± 1	244 ± 1	21 ± 1	25 ± 1
L2	132 ± 2	241 ± 3	21 ± 1	23 ± 2

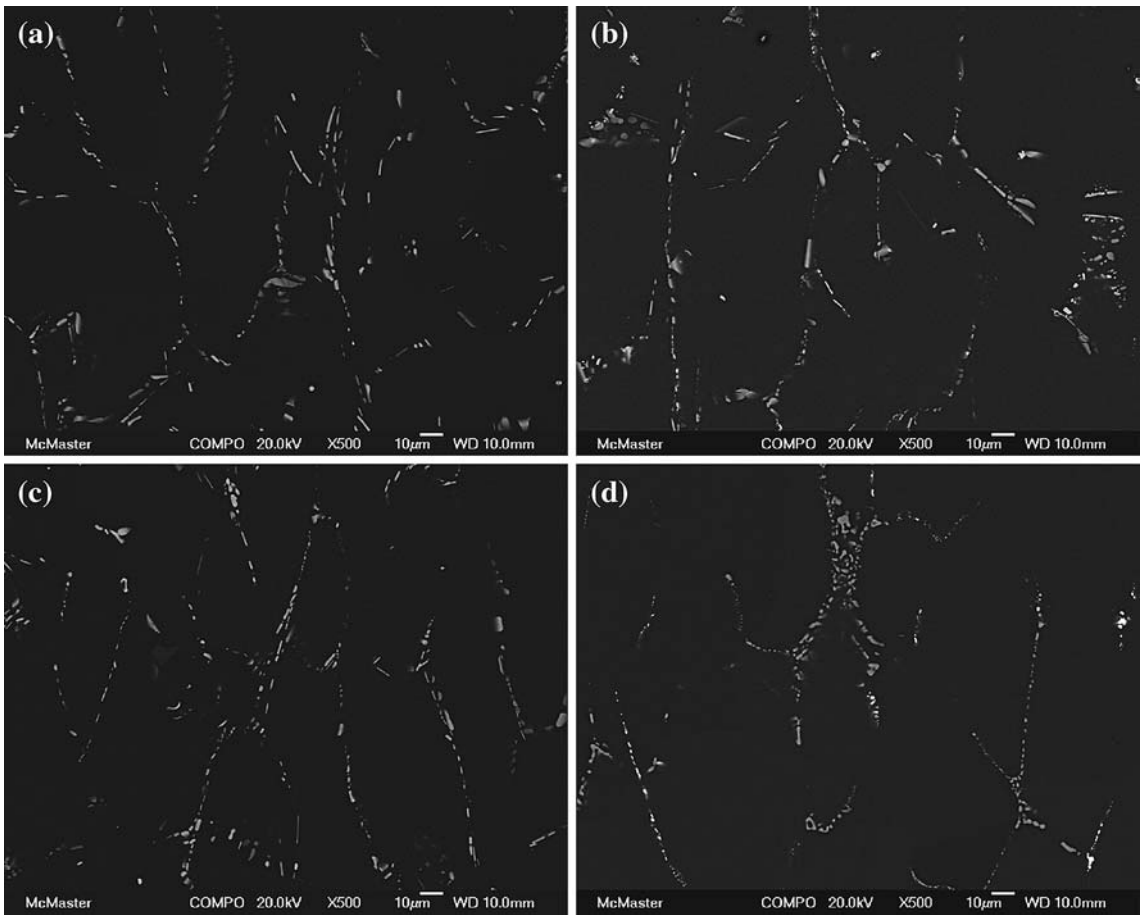

Fig. 8 Backscattered image of **a** RC, **b** C1, **c** RL, and **d** L2 alloys in T4 temper

Table 6 Grain size of the alloys in T4 temper measured in transverse plane

Alloy	Grain size (mm)	
	Transverse plane	
	t(0°)	t(90°)
RC	0.76 ± 0.07	0.26 ± 0.03
C04	0.56 ± 0.05	0.23 ± 0.02
C07	0.59 ± 0.03	0.26 ± 0.01
C1	0.60 ± 0.05	0.26 ± 0.02
C2	0.72 ± 0.09	0.27 ± 0.02
RL	0.65 ± 0.05	0.28 ± 0.02
L04	0.59 ± 0.04	0.27 ± 0.03
L07	0.74 ± 0.03	0.26 ± 0.02
L1	0.69 ± 0.04	0.24 ± 0.02
L2	0.64 ± 0.05	0.25 ± 0.02

the addition of Sr to 6061 alloy. They arrived at the same conclusion that there was no difference between modified and Sr-free alloys after thermo-mechanical processing. However, it was possible to extrude Sr-modified alloys at higher rates and the homogenization time prior to extrusion was reduced. It is expected that La addition also leads to improvements in the thermo-mechanical processing and heat treatment of the alloy. This issue needs to be clarified by further investigation.

Conclusions

1. An addition of 0.1–0.2 wt.% of lanthanum to an experimental 6xxx series Al alloy is shown to have beneficial effects on the alloy in the as-cast condition. Firstly, it promotes the formation of Chinese script α-AlFeSi phase at the expense of harmful β platelet-type particles. Secondly, the grain size of the alloy uniformly decreases with the increase in La content.
2. It was anticipated that Ce and La would demonstrate slightly dissimilar modifying abilities due to existing yet non-crucial differences in their chemical and physical properties. In spite of that expectation, these two rare-earth metals demonstrate disparate modifying potency: while lanthanum suppresses the formation of

the β phase in as-cast alloys and reduces the grain size, cerium additions are totally inefficient in this respect.

3. Since neither La nor Ce dissolves in the Fe-bearing intermetallics present in modified alloys, a modification mechanism related to surface adsorption is more likely. Surface adsorption of La to the interface of α prevents Si diffusion into this phase which is needed for its transformation to β.
4. Ce-containing and La-containing particles were seen in Ce-added and La-added alloys, respectively. EDS examination showed that iron was not a constituent of these phases.
5. Despite beneficial changes that La addition had on the alloy in as-cast condition, no improvement in the bendability of the alloy was observed after thermo-mechanical processing. It was found that the break-down of intermetallics during rolling and solutionizing processes eliminated the differences between the microstructure of the reference and La-added alloy samples. Furthermore, the dynamic recrystallization accompanying hot rolling and grain growth during solutionizing resulted in the same grain size in all alloys. The similarity of microstructure and grain size was reflected in the similar bendability of reference and La-treated alloys.

Acknowledgements The authors gratefully acknowledge the financial support of the Auto 21 research initiative. The in kind support of Novelis Inc. is also greatly appreciated.

References

1. Spencer K, Corbin SF, Lloyd DJ (2002) Mater Sci Eng A 325:394
2. Lievers WB, Pilkey AK, Lloyd DJ (2003) Mater Sci Eng A 361:312
3. Musulin I, Celliers OC (1990) In: Light metals 1990 proceedings of the 119th TMS annual meeting, pp 951–954
4. Clode MP, Sheppard T (1990) Mater Sci Technol 6:755
5. Onurlu S, Tekin A (1994) J Mater Sci 29:1652
6. Zajac S, Hutchinson B, Johansson A, Gullman LO (1994) Mater Sci Technol 10:323
7. Birol Y (2004) J Mater Process Tech 148:250
8. Couto KBS, Claves SR, Van Geertruyden WH, Misiolek WZ, Goncalves M (2005) Mater Sci Tech 21:263
9. Shabestari SG, Gruzleski JE (1995) Trans AFS 26:285
10. Mulazimoglu MH, Zaluska A, Gruzleski JE, Paray F (1996) Metall Mater Trans 27A:929
11. Paray F, Kulunk B, Gruzleski J (1996) Mater Sci Tech 12:315
12. Samuel FH, Samuel AM, Doty HW, Valtierra S (2001) Metall Mater Trans 32A:2061
13. Bakke P, Pettersen K, Westengen H (2003) JOM 55:46
14. Pekguleryuz MO, Kaya AA (2003) Adv Eng Mater 5:866
15. Xia Z, Chen Z, Shi A, Mu N, Sun N (2002) J Electron Mater 31:564
16. Lawrence CM, Wu CML, Yu DQ, Law CMT, Wang L (2002) J Electron Mater 3:921
17. Morris DG, Chao J, Garcia Oca C, Munoz-Morris MA (2003) Mater Sci Eng A 339:232
18. Salazar M, Perez R, Rosas G (2003) Mater Sci Forum 426–432:1837
19. Fu H, Xiao Q, Li Y (2005) Mater Sci Eng A 395:281
20. Cao Z, Sun D, Du W, Zheng Z (1990) Aluminum alloys: their physical and mechanical properties. In: Proceedings of 2nd international conference, pp 312–314
21. Ravi M, Pillai UTS, Pai BC, Damodaran AD, Dwarakadasa ES (2002) Metall Mater Trans 33A:391
22. Bryant JD (1999) Metall Mater Trans 30A:2006
23. Abu Khatwa MK, Malakhov DV (2006) CALPHAD 30:159
24. Datsko J, Yang CT (1960) J Eng Ind 82:309
25. Liu Z, Chang YA (1999) Metall Mater Trans 30A:1081
26. Hansen V, Hauback B, Sundberg M, Rumming C, Gjùnnes J (1998) Acta Crystallogr B 54:351
27. Ashtari P, Tezuka H, Sato T (2004) Scr Mater 51:43
28. Ashtari P, Tezuka H, Sato T (2005) Scr Mater 53:937
29. Backerud L, Krol E, Tamminen J (1986) Solidification characteristics of aluminum alloys vol 1: wrought alloys. SkanAluminum, Sweden
30. Mondolfo LF (1978) Manganese in aluminium alloys. Page Bros. (Norwich) Ltd., England
31. Barlock J, Mondolfo L (1975) Z Metallkd 66:605
32. Zakharov AM, Gul'din IT, Arnol'd AA, Matsenko YuA (1989) Russ Metall 4:209